Remote Sensing Applications: Society and Environment 8 (2017) 71–82

Contents lists available at ScienceDirect

Remote Sensing Applications: Society and Environment

journal homepage: www.elsevier.com/locate/rsase

Fire disturbance data improves the accuracy of remotely sensed estimates of aboveground biomass for boreal forests in eastern Canada

Dinesh Babu Irulappa Pillai Vijayakumar[a,*], Frédéric Raulier[a], Pierre Bernier[b], Sylvie Gauthier[b], Yves Bergeron[c], David Pothier[a]

[a] Centre d'Étude de la Forêt, and Faculté de Foresterie, de Géographie et de Géomatique, Université Laval, 2405 rue de la Terrasse, Terrasse, Québec, QC, Canada G1V 0A6
[b] Natural Resources Canada, Canadian Forest Service, Laurentian Forestry Centre, 1055 du P.E.P.S., P.O. Box 10380, Sainte-Foy Stn.,Stn., Québec, QC, Canada G1V 4C7
[c] Institut de recherche sur les forêts, Université du Québec en Abitibi-Témiscamingue, 445 boulevard de l'Université, Rouyn-Noranda, QC, Canada J9× 4E5

ARTICLE INFO

Keywords:
Aboveground biomass
Boreal forests
Remote sensing
Successional dynamics
MODIS
GLAS
ASAR

ABSTRACT

Accurate estimation of aboveground biomass (AGB) using remote sensing data is still challenging and an approach based on an understanding of forest disturbance and succession could help improve AGB estimation. In the boreal forest of North America, time since last fire (TSLF) is seen as a useful variable to explain post-fire successional change and aboveground biomass (AGB). Within a large study area (> 200 000 km^2) located in the northeastern American boreal forest, we compared remotely sensed biomass estimates of MODIS (Moderate Resolution Imaging Spectroradiometer), GLAS (Geoscience Laser Altimeter System) and ASAR (Advanced Synthetic Aperture Radar) with inventory-based estimates derived from ground plots, and forest maps at a spatial resolution of 2-km^2. We identified that TSLF could explain the error observed in remotely sensed AGB estimates (MODIS (45%), GLAS (47%) or ASAR (23%)) when associated with surficial geological substrate information at that scale. Our results therefore show the importance of TSLF as a potential ancillary variable for improving the accuracy of remotely sensed AGB estimates in North American boreal forests.

1. Introduction

Forested biomes cover approximately 3.7 billion ha (FAO, 2015), and contribute significantly to the global carbon (C) cycle (McGuire, 2002), notably circumboreal forests (32% of global forest carbon stocks, Pan et al., 2011). In a recent study, Bradshaw and Warkentin (2015) reported total carbon stocks of 367.3–1715.8 Pg (midpoint = 1095 Pg), which are about 3.8 times those estimated by Pan et al. (2011) for boreal forests. These considerable differences indicate that improvement is still required to increase the accuracy of C stock estimates. Information on aboveground biomass (AGB) is used for assessing forest ecosystem productivity (Malhi, 2012), and for supporting bio-energy production (Mansuy et al., 2015).

Maps of AGB derived from remote sensing are fundamentally based on the pixel-level application of empirical models relating spectral reflectance data to field measurements of biomass, themselves derived from tree-level measurements and allometric equations or biomass expansion factors. Various sensors have different operating potentials and constraints. More specifically, optical multispectral imagery (e.g. Moderate Resolution Imaging Spectroradiometer, MODIS) and short-wavelength radar data (e.g. C-band Advanced Synthetic Aperture Radar, ASAR) are limited by saturation regions of high biomass and complex canopy structures (Turner et al., 1999; Pflugmacher et al., 2012). LiDAR (Light Detection and Ranging) based active remote sensing technologies can measure canopy height and crown dimensions directly, through measurements of distance between the sensor and target (Drake et al., 2003), thereby overcoming data saturation in biomass estimation (e.g., Geoscience Laser Altimeter System (GLAS) sensor, Zhang et al., 2014a; Zhang et al., 2014b).

The comparisons of biomass maps from different sources of remote sensing data may also provide useful information from which more accurate AGB estimates can be derived (e.g., Avitabile et al., 2011; Mitchard et al., 2013, Mitchard et al., 2014). Hill et al. (2013) found only low correlations between the various estimates, from nine different studies (e.g., Saatchi et al., 2011; Baccini et al., 2012) based on MODIS and GLAS data acquired across tropical forests at the extent of continental Africa.

Ground data is also often insufficient to properly estimate errors in remotely sensed estimates (Hill et al., 2013; Mitchard et al., 2014). The addition of prior vegetation recovery trends, disturbance histories, and known forest structural attributes to remote sensing data is known to improve the accuracy of biomass estimation (Main-Knorn et al., 2011;

* Corresponding author.
E-mail address: dinesh-babu.irulappa-pillai-vijayakum.1@ulaval.ca (D.B. Irulappa Pillai Vijayakumar).

http://dx.doi.org/10.1016/j.rsase.2017.07.010
Received 5 June 2017; Received in revised form 15 July 2017; Accepted 30 July 2017
Available online 02 August 2017

Pflugmacher et al., 2014). However, remotely sensed AGB estimates seldom consider the spatial knowledge of recorded disturbances and recovery patterns of the forest under study (Chu and Guo, 2014).

In North American boreal ecosystems, changes in C storage over time are related to fire events (Harden et al., 2000), which are highly stochastic in both time and space (Girardin et al., 2013). A disturbance regime may be characterized by disturbance frequency, size and severity (Bergeron et al., 2002). Small fires are most frequent, but infrequent large fires predominantly shape the boreal landscape mosaic (Johnson et al., 1998; Bergeron et al., 2004). Time since last fire (TSLF) is the most significant predictor of postfire canopy recovery (Mansuy et al., 2012), which is itself related to changes associated with forest structural attributes over time (e.g. canopy cover) that control AGB at the scale of landscapes (Irulappa Pillai Vijayakumar et al., 2016). However, burn severity varies inside fire perimeters (Johnstone et al., 2010; Jin et al., 2012), blurring the relationship between disturbance history, post-fire canopy recovery and AGB (Lecomte et al., 2006; Chaieb et al., 2015). Biomass estimation must therefore be done at a scale that matches that of the dominant disturbance, namely fire (Frolking et al., 2009).

The objectives of this study were 1) to compare biomass (AGB) maps derived from MODIS, GLAS, and ASAR with those obtained from an AGB model based on ground-inventory data amassed over a large area of the boreal forest in eastern Canada, and 2) to assess if the error observed with remotely sensed AGB estimates (differences between inventory-based AGB and remotely sensed AGB estimates) can be explained by TSLF, vegetation cover and geological substrate information.

We obtained AGB estimates based on MODIS and ASAR data collected for the study area from Beaudoin et al. (2014) and Thurner et al. (2014), respectively. We developed an AGB model for GLAS data following a methodology successfully developed by Zhang et al. (2014b). We compared these estimates with those of an inventory-based AGB map (Irulappa Pillai Vijayakumar et al., 2016) elaborated from aerial photo-interpreted stand maps and a large number of forest inventory plots.

2. Material and methods

2.1. Study area

The region (Fig. 1) selected for this study is situated in eastern Canada (49°N to 52°N and 66°W to 79° 30'W, area: 217,000 km^2), and is entirely included within the boreal black spruce (*Picea mariana* (Mill.) BSP) -moss bioclimatic domain (Robitaille and Saucier, 1998). This choice was based on the availability of fire history maps and forest inventory data. The study area can be divided into a western and an eastern regions that differ in biophysical environments and consequently in fire regime and vegetation. The western region has an annual precipitation of 700 mm y^{-1}and a mean annual temperature of −0.65 °C (Robitaille and Saucier, 1998). It characterized by relatively short fire return intervals (270 years; Bergeron et al., 2004) and its landscapes are dominated by post-fire tree species such as black spruce, jack pine (*Pinus banksiana* Lamb.) and, to a lesser extent, by white birch (*Betula papyrifera* Marsh.) and trembling aspen (*Populus tremuloides* Michx.). The eastern region shows a wetter and cooler climate with an annual precipitation between 1000 and 2000 mm y^{-1} and a mean annual temperature of −1.5 °C (Saucier et al., 2009). Fire return intervals are thus longer (> 500 years; Bouchard et al., 2008) and landscapes host abundant fire-averse balsam fir (*Abies balsamea*[L.]Mill.), mixed with black spruce.

2.2. General design

A general flow diagram of the data and methods used for AGB estimation and comparison is displayed in Fig. 2.

The successive steps of our research were:

1. First, obtain the inventory, MODIS and ASAR based AGB estimates for our study region from Irulappa Pillai Vijayakumar et al. (2016), Beaudoin et al. (2014) and Thurner et al. (2014), respectively.
2. Develop a model for predicting GLAS based AGB estimates with the methodology of Zhang et al. (2014b).
3. Reproject remotely sensed AGB estimates and rescale them to a common projection and resolution.
4. Compute the differences between inventory-based and remotely sensed AGB estimates.
5. Explain the observed differences between inventory-based and remotely sensed estimates using TSLF, vegetation cover information and geological substrate information.

We used for our model building process (steps: 2 and 5) non-parametric model Random Forests (RF). RF is a supervised learning algorithm that develops non-parametric models without making any assumption on the underlying distribution of the data. It randomly subsamples data (bootstrap) such that 63% of data is utilized for training and the remaining data is used for cross-validation. For each bootstrap sample from the training data, decision trees are constructed by choosing the best predictor variables to split data into homogenous

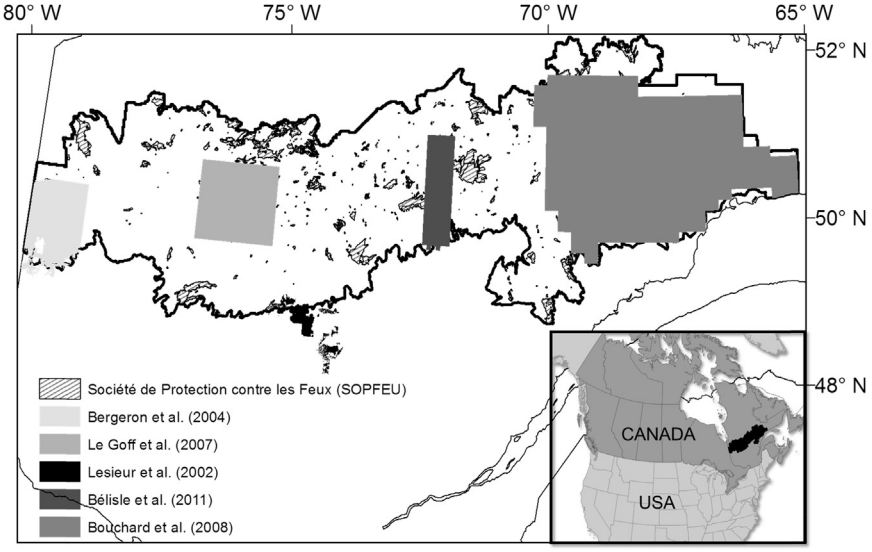

Fig. 1. Locations of the study area (dark outline) and training datasets (grey areas) from the published studies (Le Goff et al., 2007 and Lesieur et al., 2002).

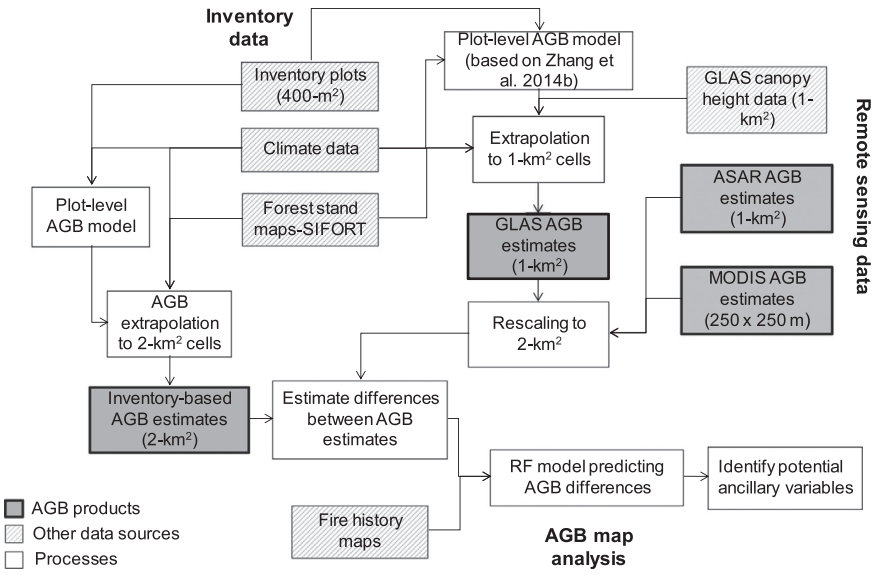

Fig. 2. General flow diagram.

sets based on least mean square error. Decision trees are grown until there is no more significant improvement in accuracy. Finally, aggregation of decision trees is used for predictions. We used the following settings for each bootstrap iteration of RF models: 1), the number of decision trees constructed during each run (*ntree*) was fixed to 1000; 2), the number of predictor variables taken for constructing each tree node (*mtry*) was set to one third of the number of variables choosed for fitting a RF model; 3), the minimum size of the terminal nodes (*node size*) was fixed to 5.

We developed RF models using the *randomForest* package for R (Liaw and Wiener, 2002). The predictors for fitting RF modelswere selected using the *Boruta* package in R (Number of iterations = 1000; number of trees = 1000) (adapted from Kursa and Rudnicki, 2010). We selected the six most important variables assessed by *Boruta* to fit parsimonious and robust models (Thompson and Spies, 2009). Correlation analyses were performed to detect collinearity between the selected predictors (threshold: $r > 0.70$, Dormann et al., 2013) to avoid problems of multicollinearity.

2.2.1. Estimation of AGB based on inventory data

We used the inventory-based AGB estimates of Irulappa Pillai Vijayakumar et al. (2016) in which AGB values were estimated at a spatial resolution of 2-km^2 (1414 m × 1414 m). This cell-size corresponds to the minimum size for large fires included in the Canadian large fire database. These large fires account for 97% of the total area burned between 1959 and 1999 (Stocks et al., 2003). This resolution also seemed adequate to circumvent confounding issues typically found with finer resolution, such as the variation of post-fire forest recovery patterns within burned areas due to the within-fire variability of fire severity (Jin et al., 2012) and neighboring effects (Frelich and Reich, 1999).

Values of aboveground biomass carbon (ABC, being equal to 50% of AGB, Gower et al., 1997) were first obtained from inventory plots (temporary sample plot database; 400-m^2, 1992–2003), and then successively scaled to 14-ha tesserae and to 2-km^2 cells, as in Irulappa Pillai Vijayakumar et al. (2016). Key to this scaling exercise was the availability of spatially explicit forest stand properties across the study area with the SIFORT geospatial database (Spatial Information on Forest Composition based on Tesserae, Pelletier et al., 2007) originating from forest maps (1:15,000 scale) and elaborated by the Quebec Ministry of Natural Resources between 1990 and 1999 for its third inventory program (1992–2002). The SIFORT database consists of a mosaic of square tiles each covering an average area of 14 ha to which were attributed the forest properties values of the stand located at the tile centroid from inventory-based forest maps. Tiles whose centroids fell on wetlands and peatlands, water, heaths, harvested land, insect-killed stands or windthrows and human infrastructure were excluded from the Irulappa Pillai Vijayakumar et al. (2016) dataset, leaving 89% of the study area, or about 193,000 km^2, to be used for AGB estimation.

A RF model of ABC ($r^2 = 0.50$, RMSE = 13.88 Mg ha^{-1}) was trained at the plot level by Irulappa Pillai Vijayakumar et al. (2016) using estimated ABC values and observed forest attributes and climate variables. This model was then used on all SIFORT tile centroids within a training dataset, and the resulting estimates were then averaged among tile centroids within 2-km^2 cells to train another non-parametric RF model at 2-km^2 spatial resolution ($r^2 = 0.83$, RMSE = 0.28 Gg km^{-2}) with the objective of obtaining spatially continuous ABC estimates at the 2 km^2 spatial resolution for the whole study area. This training dataset included all areas for which a TSLF value could be provided from contemporaneous or historical fire maps and covered 43.8% of the present study area (Fig. 1). Relative proportions of canopy cover density classes were the main variables influencing ABC estimates at the 2-km^2 spatial resolution. More detailed information is found in Irulappa Pillai Vijayakumar et al. (2016).

2.2.2. Estimation of AGB from remote sensing data

We used three remote sensing data products (MODIS, GLAS and ASAR) to estimate biomass at the 2-km^2 scale. We selected these three data sources to consider the most common types of sensors (passive [optical multi-spectral] and active [radar and laser scanner]) used for AGB estimation (Lu et al., 2014).

We first calibrated an AGB model with spaceborne GLAS LiDAR canopy height data (Simard et al., 2011) by adapting the methodology developed by Zhang et al. (2014b). Plot-level AGB values ($n = 8739$, third forest inventory [1992–2003], Ministry of Natural Resources of Quebec) were estimated by converting diameter at breast height (DBH, 1.3 m) into biomass using species-specific allometric equations for commercial tree species (Lambert et al., 2005; Ung et al., 2008), non-commercial tree species (Ter-Mikaelian and Korzukhin, 1997), and shrubs (Buech and Rugg, 1989). These estimates were summed at the plot level. A random forest (RF) model was then developed to estimate plot-level AGB from observed canopy height (dominant height of the canopy, i.e., mean height of the dominant trees; Burkhart and Tomé, 2012), elevation and climate variables (Compo et al., 2011) (Table 1). This model was then used to predict AGB across the study region using the GLAS canopy height data at 1 km resolution. We tested for spatial autocorrelation in model residuals to detect potential omission of important variables (Dormann et al., 2007). To this end, we computed

Table 1
List of explanatory variables that were used to estimate AGB.

Relative frequencies of vegetation variables[a]	Physical site variables	Climate variables[b]
Species composition groups - Black spruce, balsam fir, jack pine, intolerant hardwoods, mixed, other conifers and no species composition but identified as a burned area, following Gauthier et al. (2010).	Surficial deposit groups[a] –VAVC (very abundant, very coarse), MM (moderate, moderate), MAM (moderately abundant, moderate), MAC (moderately abundant, coarse), AC (abundant, coarse), ROC (rock) and ORG (organic) (Mansuy et al., 2010).	Temperature (°C) –mean annual temperature Total precipitation (mm $year^{-1}$) –the mean of annual total precipitation
Stand age classes − 0 to 20 years, 21–40, 41–60, 61–80, 81–100, ≥ 101; young uneven-aged, and old uneven-aged.	Elevation (m) - Derived for study units from SRTM DEM (90 m resolution) (Van Zyl, 2001).	Degree-days (°C $year^{-1}$) – Annual growing degree-days sum (above 5 °C) Growing season length (days $year^{-1}$) –Duration of days for which the mean temperature is above 5 °C
Stand height classes - > 22 m, 17–22 m, 12–17 m, 7–12 m, 4–7 m, 2–4 m, and 0–2 m.	Slope (°) - derived from elevation data in ArcGIS 10.0	Potential evapotranspiration (mm) – Annual total potential evapotranspiration (PET, Dunne and Leopold, 1978)
Stand cover density classes - > 81%, 61–80%, 41–60%, and 25–40%.		Aridity index (mm $year^{-1}$) –Accumulated monthly water deficit (monthly Thornthwaite potential evapotranspiration minus monthly precipitation) Canadian drought code – Moisture content of the deep compacted organic matter layer, 10–20 cm depth (Amiro et al., 2001)

[a] Derived from SIFORT geospatial database.
[b] Derived from the 20CR project (Compo et al., 2011) with BioSIM (Régnière and St-Amant, 2008) for the period of 1971–2000.

Global Moran's *I*, an index of spatial autocorrelation, as a function of neighbouring distance (Moran, 1950).

We then extracted MODIS based AGB values for our study region from the Canada-wide AGB spatial productof Beaudoin et al. (2014). The authors mapped AGB at 250 × 250 m pixel resolution as a function of MODIS spectral reflectance, climatic and topographic variables using Canada's National Forest inventory photo-plots (2 km × 2 km) (Gillis et al., 2005) and a *k* nearest-neighbour (*k*NN) method. Each 2 km × 2 km photo-plot consisted of forest polygons characterized by cartographic attributes of vegetation composition, stand structure, and AGB information based on the models of Boudewyn et al. (2007). They rasterized AGB information from photo-plots to the 250 m × 250 m MODIS grid and used these photo-plot pixels as references to impute AGB values to the rest of the study area.

We further obtained an AGB map based on ASAR data from Thurner et al. (2014). This AGB map covers the Northern Hemisphere between 30°N and 80°N for boreal and temperate forests of North America, Europe and Asia. It is based on estimates of growing stock volume (volume of tree stems per unit area, m^3 ha^{-1}) obtained with the BIOMASAR retrieval algorithm developed for the Envisat/ASAR satellite data at a spatial resolution of 0.01° (Santoro et al., 2011). BIOMASAR is an automated approach for modeling growing stock volume as a function of radar backscatter. This technique is based on how forest structural properties affect the response of a radar signal. Volume estimates were then converted to biomass. A more detailed explanation of this product is given by Thurner et al. (2014).

We reprojected these biomass products of different resolution (1 km^2, GLAS biomass map; 250 m × 250 m, MODIS biomass estimates, Beaudoin et al., 2014; and 0.01° resolution, ASAR biomass estimates, Thurner et al., 2014) to the same projection (North American Datum 1983; Lambert conformal conic projection) employing a nearest neighbor resampling technique. We then performed a spatial aggregation by computing the mean value of remotely sensed AGB values for pixel centers located within each 2-km^2 cell, the scale of inventory-based estimates.

2.2.3. Comparison of biomass maps

Our comparison analysis is affected by the physical principles of data acquisition used in sensors and by the spatial resolution used for the comparisons. Comparison of these products at a finer scale resolution was not considered so as to match the scale from which large fire disturbances start to impact the forest landscape structure on a regional scale (e.g. Johnson and Gutsell, 1994: Fig. 5; Frolking et al., 2009). The inventory-based AGB map of Irulappa Pillai Vijayakumar et al. (2016) was therefore of limited use to validate remote sensing products, but was useful to show agreement or disagreement in the spatial trends observed between remotely sensed and inventory-based estimates over a large area. We considered a departure from the inventory-based map as an error (i.e. a disagreement). Values of errors were used to test the use of TSLF and other ancillary variables for improving AGB estimates from satellites over large areas.

We first explored covariations between each of the GLAS, MODIS, ASAR and inventory-based estimates in the training dataset using the Pearson correlation coefficient accounting for spatial autocorrelation in the *SpatialPack* package for R. We calculated the difference between each of the GLAS, MODIS and ASAR-based AGB estimates, and the inventory-based estimates of AGB for each 2-km^2cell in the training dataset to identify potential ancillary variables. To this end, we used the training dataset created by Irulappa Pillai Vijayakumar et al. (2015). This training dataset consists of 34,234 2-km^2cells. Cells were included in this dataset for one of the following three reasons:50% or more of the area of a 2-km^2 cell was covered by a recent fire polygon (1970–2000, from the SOPFEU, i.e. the Quebec forest fire control agency, Société de protection des forêtscontre le feu) or by a fire polygon from history maps (1880–2000) (Fig. 1). In addition, cells were included if they had more than one inventory plot (third inventory program [1992–2003], Ministry of Natural Resources of Quebec) dominated by post-fire tree species (paper birch, trembling aspen, jack pine, black spruce) and even-aged (oldest plot age was used as TSLF) (Bélisle et al., 2011).

We then developed RF models relating these map differences to covariates (relative cell frequencies of SIFORT attributes, Table 1) and observed TSLF at the 2-km^2 scale. We also included indices of surficial deposits in the models based on the results of Asner et al. (2010). Results of these non-parametric models are difficult to interpret and synthesize. For this reason, we also analyzed the variation in remotely sensed AGB estimates as a function of observed TSLF at the 2-km^2 scale, which is equivalent to producing AGB yield curves. This was intended to provide insights on the relationship existing between remotely sensed biomass estimates and TSLF at the scale of 2-km^2.

3. Results

3.1. Estimation of AGB with GLAS canopy height data

AGB was moderately correlated with ground-measured canopy height at the plot level ($r = 0.43$, $P < 0.01$). Variable importance rating with the *Boruta* procedure further indicated that at that level, AGB was also related to potential evapotranspiration (PET), precipitation,

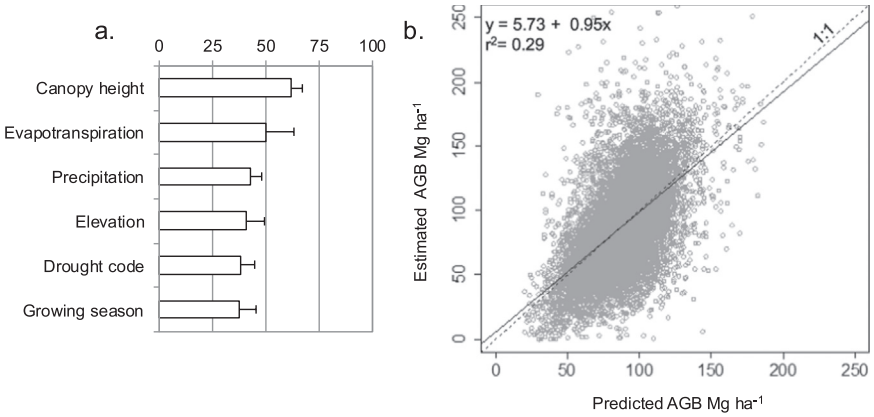

Fig. 3. Top six variables that were ranked by a random forest model for estimating AGB, based on observed canopy height at plot level (a); (b) density plot of observed vs predicted AGB by the model based on observed canopy height at plot level.

elevation, drought code, and growing season length (Table 1, Fig. 3a). Elevation was not included given its strong correlation with growing season length ($r = -0.82$, $P < 0.01$). Overall, the prediction accuracy of AGB remained moderate (i.e. $r \in [0.33, 0.66]$) ($r = 0.54$, RMSE = 33.21 Mg ha^{-1}; Fig. 3b). Residuals were weakly spatially autocorrelated (Global Moran's I statistic = −0.05, for distances < 20 km). With this RF, we extrapolated AGB to the entire landscape using GLAS canopy height data at 1-km resolution.

3.2. Covariation of remotely sensed and inventory-based biomass estimates

AGB maps from MODIS and ASAR showed an expected pattern of high and low values along an east-west gradient (Fig. 4b, d), in relation with the fire regime gradient observed over the study area. Spatial distributions of AGB estimated with MODIS and inventory-based data also agreed with one another. When the inventory-based and MODIS AGB maps were compared visually with fire disturbance history, both showed low biomass values in recently burned areas (Fig. 4a, b). The AGB estimates from ASAR also showed a similar degree of spatial agreement but with lower values in recently burned areas (Fig. 4d). The GLAS biomass map exhibited a very different spatial pattern of low and high values along a north-south gradient (Fig. 4c) that could not be associated with fire disturbance history.

When comparing remotely sensed estimates, MODIS estimates exhibited the greatest correlation with inventory-based estimates ($r = 0.56$, $P < 0.01$, RMSE = 3.28 Gg km^{-2}; Fig. 5b), when compared to GLAS ($r = 0.51$, $P < 0.01$, RMSE = 2.45 Gg km^{-2}; Fig. 5a) or ASAR estimates ($r = 0.28$, $P < 0.01$, RMSE = 4.04 Gg km^{-2}; Fig. 5c).

Correlations among remotely sensed AGB estimates of MODIS, GLAS and ASAR were also moderate: ASAR vs GLAS, $r = 0.38$, $P < 0.01$, RMSE = 4.15 Gg km^{-2} (Fig. 6a); ASAR vs MODIS, $r = 0.56$, $P < 0.01$, RMSE = 3.26 Gg km^{-2} (Fig. 6b); GLAS vs MODIS, $r = 0.38$, $P < 0.01$, RMSE = 4.05 Gg km^{-2} (Fig. 6c). AGB estimates from GLAS data were higher, on average, than those from MODIS and ASAR (Fig. 6a, c). Table 2 reports the correlation between remotely sensed and inventory estimates after accounting for spatial autocorrelation.

3.3. Detecting potential ancillary variables for remotely sensed AGB estimations

The relative proportions of the different cover density classes within 2-km^{2}units were the most important potential ancillary variables when training RF models with differences between remotely sensed (MODIS, GLAS, ASAR) and inventory-based estimates (Fig. 7a–c). Other important variables were the relative proportions of the most dominant surficial deposits (undifferentiated tills with moderate to abundant stoniness, Table 1), and stony surficial deposits (Table 1). RF models explained 28–50% of the variability observed between remotely sensed and inventory-based estimates (MODIS, $r^2 = 0.50$, RMSE = 1.36 Gg km^{-2}; GLAS, $r^2 = 0.47$, RMSE = 1.56 Gg km^{-2}; ASAR, $r^2 = 0.28$, RMSE = 1.97 Gg km^{-2}; Fig. 7d-f).

Differences between inventory-based and remotely sensed estimates generally increased as a function of the percentage of closed cover (summed frequency of three cover density classes: > 81%, 61–80%, 41–60%) (Fig. 8a–c). TSLF is also an alternative variable (Fig. 9a–c) to reduce the disagreement existing between remotely sensed and inventory-based estimates. Indeed, the percentages of variation that was explained by models including TSLF (MODIS, $r^2 = 0.45$, RMSE = 1.36 Gg km^{-2}; GLAS, $r^2 = 0.47$, RMSE = 1.57 Gg km^{-2}; ASAR, $r^2 = 0.23$, RMSE = 2.04 Gg km^{-2}; Fig. 9d–f) were similar to those of models relying upon the relative abundances of cover density classes.

3.4. AGB yield curves with remotely sensed products

AGB yield curves based on MODIS estimates exhibited an expected trend of biomass increase as a function of TSLF until 60–90 years, and a decrease there after, which is consistent with curves based on inventory data, but with lower median values (Fig. 10a–b). AGB estimates based on GLAS data showed unexpectedly high values in recently disturbed 2-km^2 cells (TSLF < 30 years) (Fig. 10c). AGB yield curves from ASAR data exhibited a comparable trend of biomass increase as a function of TSLF (Fig. 10d), but their median values were consistently lower than GLAS, MODIS and inventory-based estimates.

4. Discussion

4.1. Interpreting covariation and spatial distributions of biomass estimates

Our analyses done at the 2-km^2 scale have shown the existence of moderate correlations between AGB estimates based on field inventory data and remotely sensed biomass estimates (Fig. 5a–c). Correlation was however lower with ASAR data, which can be explained by the fact that ASAR AGB values were estimated with relationships established at a worldwide scale (Chave et al., 2009), while GLAS and MODIS AGB estimates were partially based on forest inventory data and region-specific allometric equations.

Among the three remote sensing products, MODIS-based estimates exhibited the highest correlation with inventory-based estimates ($r = 0.56$, $P < 0.01$; Table 2). MODIS-based estimates were generated using Canada's National forest inventory photo-plots as reference data, themselves populated using provincial inventory data (Beaudoin et al., 2014). MODIS and inventory-based AGB estimates are ultimately related to provincial plot data. However, despite their moderate correlation, MODIS AGB estimates were consistently lower than inventory estimates across our training area (Fig. 10b). These differences were lower for recently disturbed cells (TSLF < 30 years) and increased with increasing TSLF, particularly for cells with a TSLF equal to 60–90 years (Figs. 9a, d, 10b). Differences were particularly high when cells had

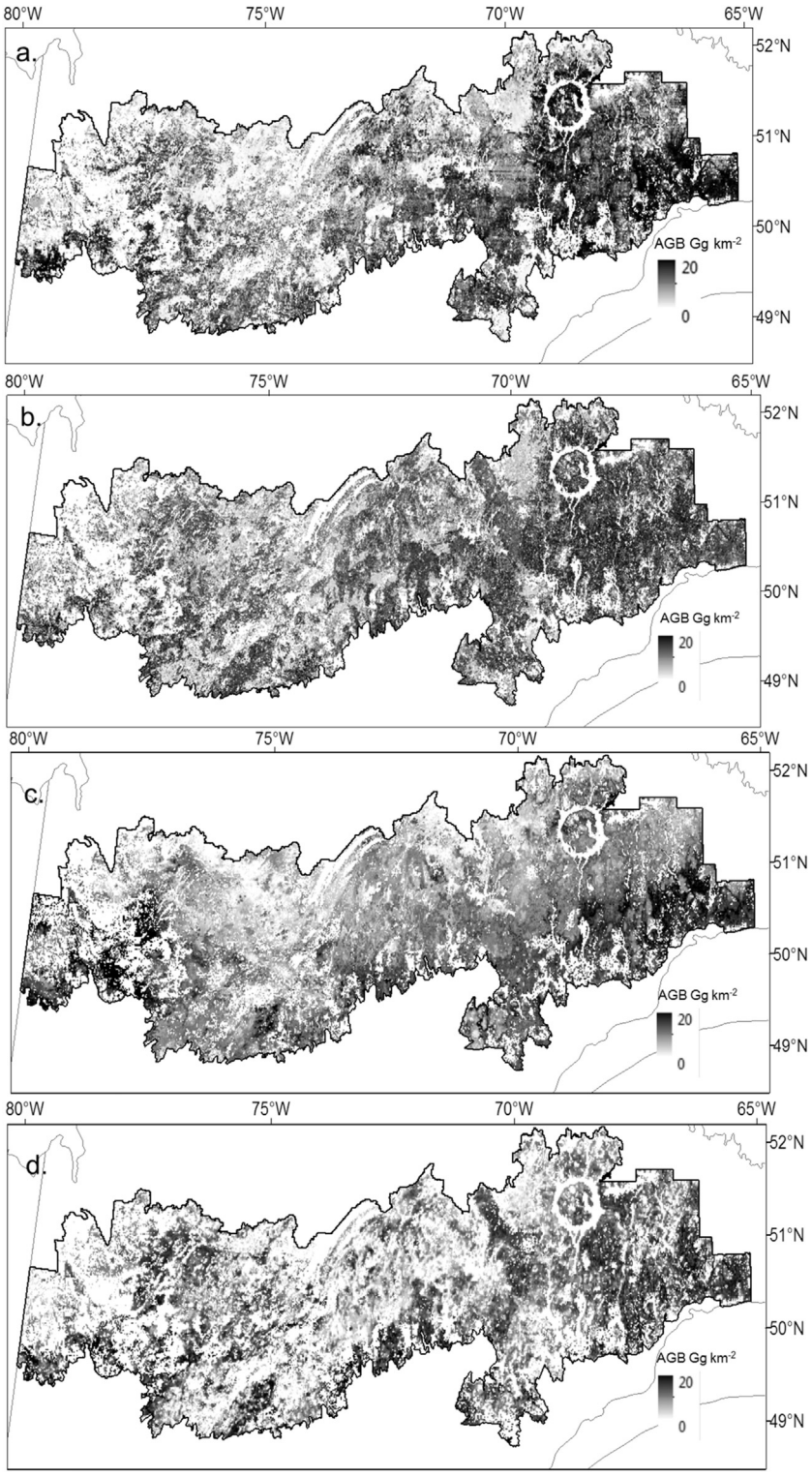

Fig. 4. Maps of AGB at the scale of 2 km^2, based upon: inventory data (a); MODIS data obtained from Beaudoin et al. (2014) (b); GLAS data (c); ASAR data obtained from Thurner et al. (2014) (d).

abundant closed canopy estimates with high biomass values (Fig. 8a; Irulappa Pillai Vijayakumar et al., 2016). The underestimation of high AGB values with MODIS has already been noted by Beaudoin et al. (2014), and more generically with the kNN method by Magnussen et al. (2010), and is related to saturation of MODIS reflectance at high biomass and the averaging effect across the k nearest neighbors.

In spite of the strong correlation found by Zhang et al. (2014b) between observed canopy height and AGB at the plot level, our estimates based on the same approach showed only a moderate correlation with observed canopy height ($r = 0.43$, $P < 0.01$). Differences in plot selection can partly explain these contrasting results, since Zhang et al. (2014b) calibrated their relationships with 75% of their plots non randomly scattered across their study area but specifically located in regions of high timber productivity. Tree species in high productivity regions are generally taller and forest stands have higher volume and biomass, where as in less productive regions, other factors, such as stand density and species composition, might also become important (Irulappa Pillai Vijayakumar et al., 2016). This would imply that

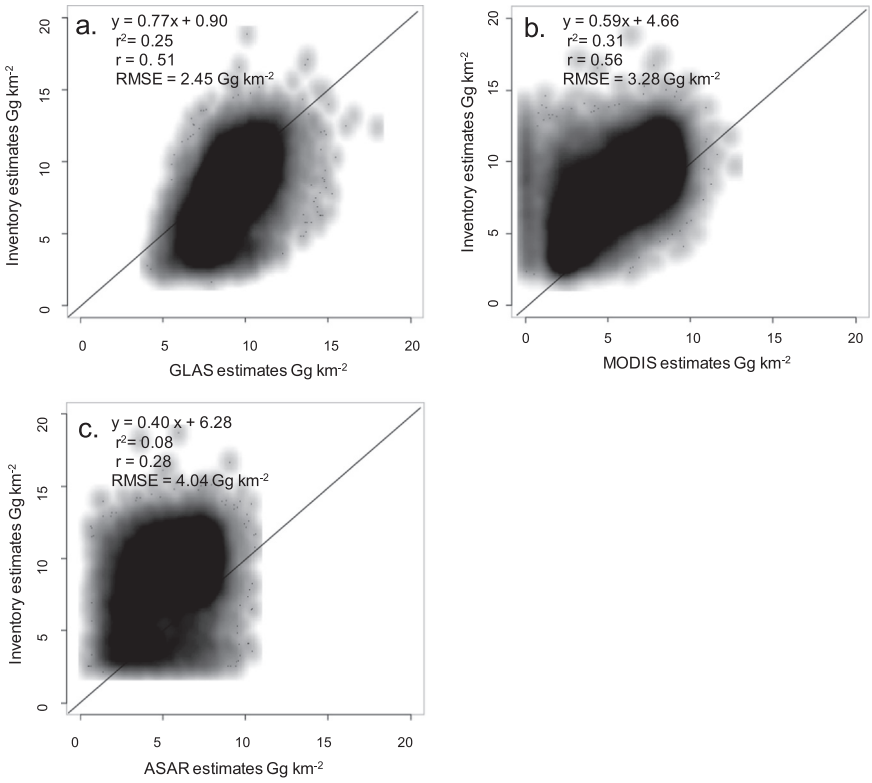

Fig. 5. Density plots of inventory-based AGB estimates as a function of remotely sensed AGB estimates at the scale of 2-km^2: (a) GLAS data; (b) MODIS data; and (c) ASAR data.

canopy height alone cannot fully explain variation of AGB variation for our region of study, which contains a wide range of site productivities.

Inventory-based AGB estimates and GLAS-measured canopy height were not correlated at the plot level in our training region ($r = -0.03$, $P > 0.05$). This lack of a relationship points to a difference of scale between forest inventory observations and GLAS acquisitions (e.g., Zhao et al., 2009). Canopy height may be an important variable to estimate biomass, but not at the spatial scale of 1 km^2, at least at the regional level. Pflugmacher et al. (2008) also suggested that GLAS estimates of biomass would be valuable on a global scale, but would differ from inventory estimates at a regional scale. As an example, Margolis et al. (2015) have reported at the continental scale for the boreal forest of North America (area, 3.7 million km^2) higher R^2 values (0.59–0.79) between inventory-based and GLAS-based AGB values, when the

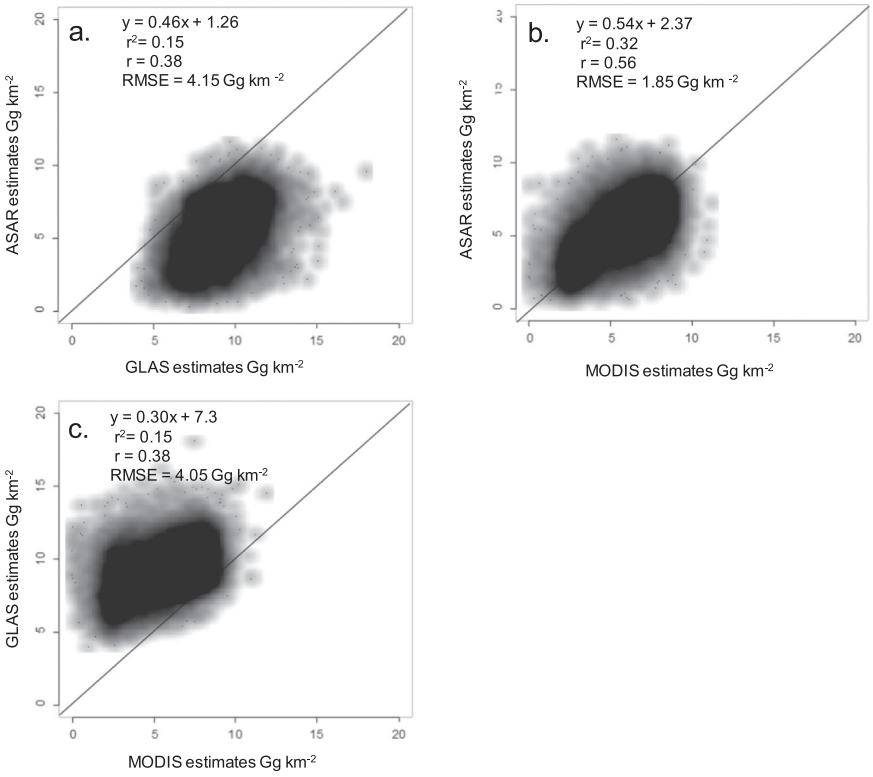

Fig. 6. Density plots of AGB estimates from remote sensing data: (a) ASAR vs GLAS; (b) ASAR vs MODIS; and (c) GLAS vs MODIS.

Table 2
Pearson correlations between each of MODIS, GLAS, ASAR and inventory-based AGB estimates after accounting for spatial autocorrelation*.

	MODIS	GLAS	ASAR
Inventory-based	0.54	0.50	0.26
MODIS		0.36	0.55
GLAS			0.37

* $P < 0.01$.

ICESAT-GLAS height metrics were used to scale up airborne LiDAR-based estimates of AGB. Because of this potential scale mismatch problem, the GLAS-derived biomass map (Fig. 4c) showed greatly contrasting spatial differences when compared to spatial patterns of AGB derived from MODIS, ASAR and inventory-based estimates. This mismatch can also explain the unexpectedly high values in areas that were recently disturbed by fire (Fig. 10c).

4.2. Consistency of results with comparable studies

Our results of moderate correlations between remotely sensed biomass estimates for boreal forests in eastern Canada agree with those from similar studies. For the Colombian Amazon forests (area of 165,000 km^2), the GLAS biomass estimates of Saatchi et al. (2011) and Baccini et al. (2012) overestimated AGB by 23% and 42% when compared to those of Asner et al. (2012) that had been derived from field plots and airborne LiDAR. Also, the GLAS biomass maps of Saatchi et al. (2011) and Baccini et al. (2012) over- or under-estimated, respectively ground-based estimates of AGB (n= 413, Amazon Forest inventory network; Malhi et al., 2002) by more than 25% and also showed different spatial patterns (Mitchard et al., 2014). The observed gradient of increasing AGB from SW to NE Amazonia was not replicated by either remote-sensed product, and it was presumed that most of the errors were related to regional variations in wood density and in height-volume relationships (Mitchard et al., 2014).

Margolis et al. (2015) compared GLAS AGB estimates of Neigh et al. (2013) with AGB estimates based on MODIS data (Beaudoin et al., 2014) for 3.7 million km^2 of the North American boreal forest. Differences in mean AGB densities between both maps (GLAS–MODIS) at the scale of World Wildlife Fund eco-regions for eastern Canadian forests and central Canadian Shield forests were 0.6 and 3.2 Mg ha^{-1}, respectively (Margolis et al., 2015, their Table 13). GLAS estimates of total eco-region AGB were consistently higher than the MODIS-based estimates of Beaudoin et al. (2014) for 16 of 18 the eco-regions in Canada (Margolis et al., 2015).

4.3. Potential ancillary variables for remotely sensed AGB estimation

Identifying that TSLF, vegetation cover and geological substrate information are able to explain 28–50% of the observed variability in the differences between remotely sensed and inventory based AGB estimates is a new observation. It means that these are potential ancillary variables for remote sensing data products when estimating AGB. At a 2-km^{2}scale, TSLF could thus serve as a proxy for canopy cover density with the benefit of possibly rectifying signal saturation in high biomass values.

Problems of scale-matching were also identified in the present study. In North American boreal ecosystems, successional dynamics are characterized by fire disturbances and post-fire vegetation recovery, both of which affect forest carbon stocks (Jones et al., 2013). Fire disturbances occur at a scale larger than most existing spatial resolutions of satellite data (Frolking et al., 2009; Bartels et al., 2016). Forest disturbance and recovery play a major role in global C budgets (Houghton, 2005). In this context, our results of showing the potential of forest succession dynamics for improving remotely sensed AGB estimates are therefore also relevant to other ecosystems (tropical and temperate). Frolking et al. (2009) have likewise emphasized the importance of combining field data with remote sensing for generating information on disturbance histories and recovery patterns to

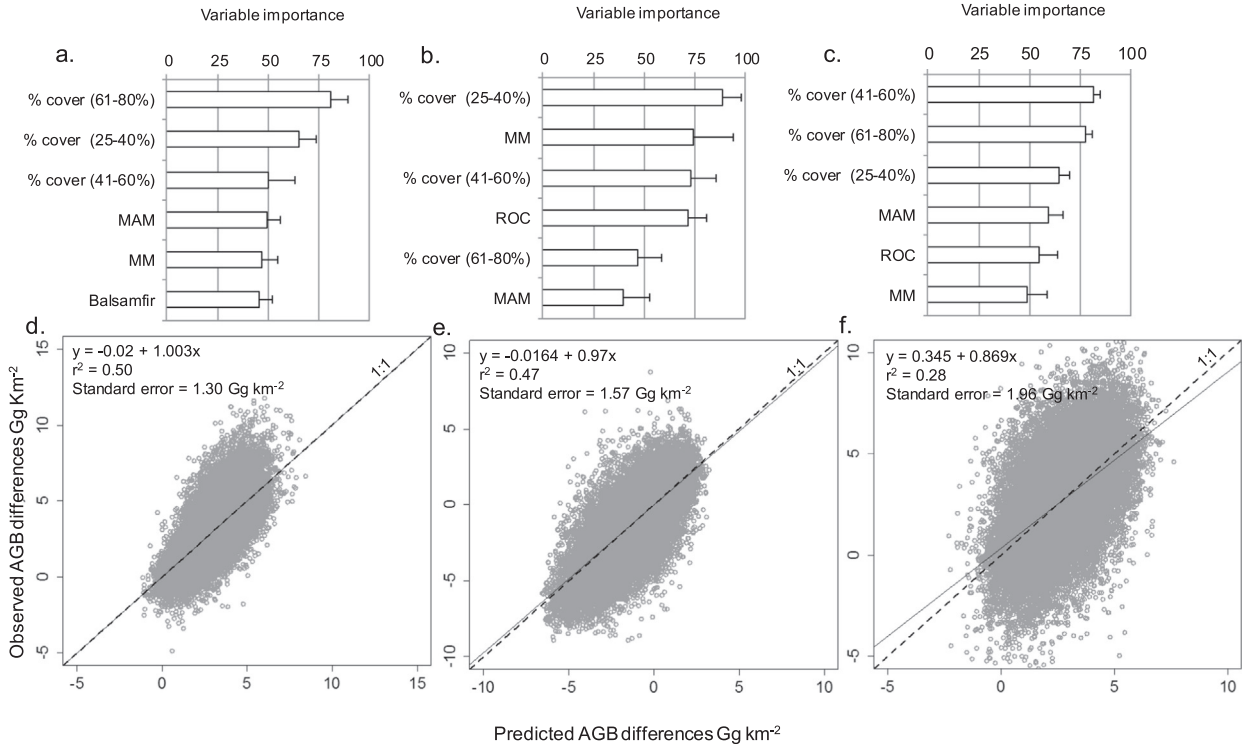

Fig. 7. Six highest ranked variables from RF models used to explain differences observed between remotely sensed and inventory-based AGB estimates with relative frequencies of SIFORT attributes (Table 1) and observed TSLF: MODIS (a); GLAS (b); and ASAR (c); density plots of observed vs predicted AGB differences between inventory-based and remotely sensed AGB estimates: MODIS (d), GLAS (e), and ASAR data (f).

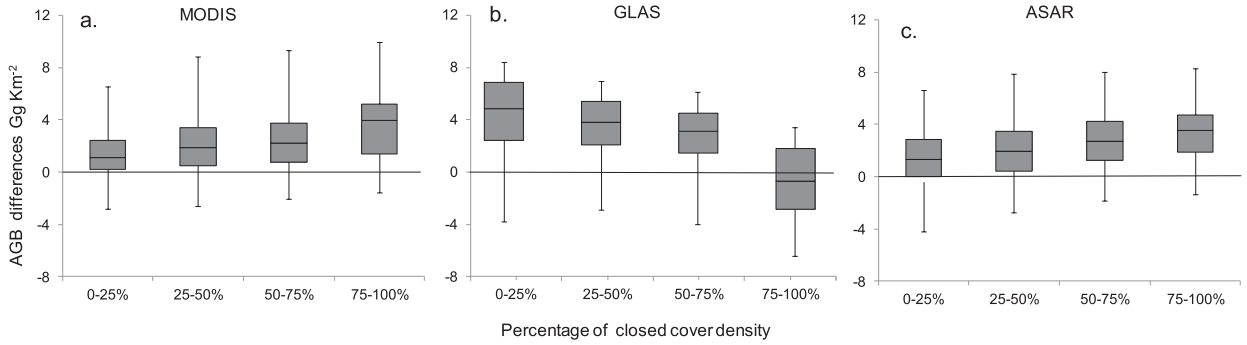

Fig. 8. Box-and-whisker plots of observed differences between inventory-based AGB estimates and biomass estimates of MODIS (a), GLAS (b), and ASAR (c), regrouped by abundance classes of closed-canopy cover densities.

accurately estimate biomass across forests world-wide. The current condition of a forest stand is related to its disturbance and recovery history (Pflugmacher et al., 2012). Time series analysis of satellite data would provide detailed information on prior canopy recovery/vegetation trend conditions that were based on disturbance histories (Main-Knorn et al., 2013; Ahmed et al., 2014; Madoui et al., 2015). Chu and Guo (2014) have proposed merging different remote sensing data with field data for generating high-quality and quantitative information on post-fire canopy recovery patterns.

5. Conclusions

We undertook this study to determine how to improve the accuracy of spatial AGB estimates based on different remote sensing data collected over a large area of boreal forest. Our analysis indicated the potential for enhancing the relationship between reflectance data and AGB through the incorporation of disturbance histories and vegetation recovery trends. Not surprisingly, adding information on the relative proportion of canopy cover density that was linked to signal saturation reduced the differences between inventory based and remotely sensed biomass estimates. TSLF may represent a proxy for such information at the 2-km^2 scale and thus presents a strong potential to rectify the problem of signal saturation.

Looking forward, the future of remote sensing of vegetation biomass relies on LiDAR technology for studying trees in a three-dimensional context. Airborne LiDAR is preferred to spaceborne LiDAR to estimate AGB, but its use remains confined to relatively small study areas due to prohibitive acquisition costs (Zolkos et al., 2013). Combining airborne LiDAR metrics with spaceborne LiDAR measurements may overcome this problem of cost (e.g. Margolis et al., 2015) and in conjunction with information on disturbance history and surficial geological substrate information may provide still more accurate AGB estimates.

Furthermore, we also have demonstrated the need to integrate ground plots with remotely sensed data up to the scale at which disturbances tend to occur. We also suggest that adequate measures of uncertainty should be provided with remotely sensed biomass estimates by using spatially exhaustive ground-plot data. We therefore propose the inclusion of metrics that relate to both horizontal and vertical

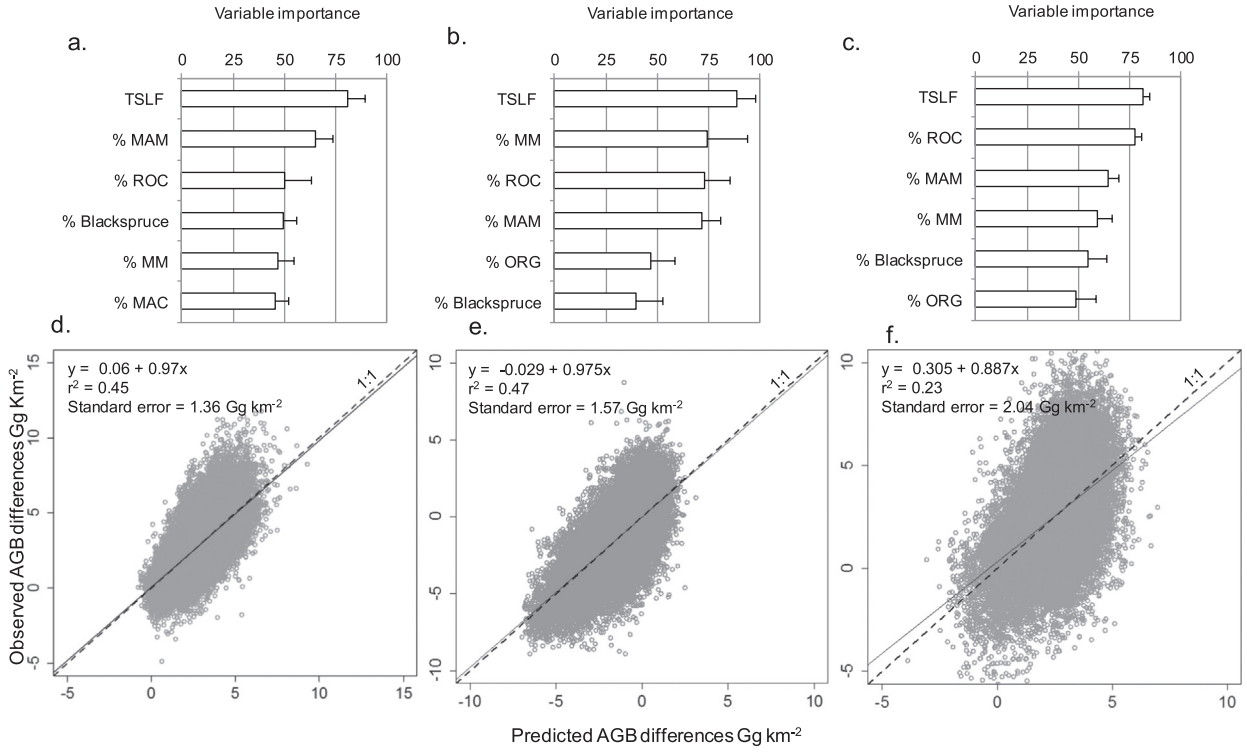

Fig. 9. Six highest ranked variables from RF models used to explain differences observed between remotely sensed and inventory-based AGB estimates when abundances of cover canopy density classes are removed from the list of potential explanatory variables: MODIS (a); GLAS (b); and ASAR (c). Density plots of observed vs predicted AGB differences between remotely sensed and inventory-based AGB estimates: MODIS (d); GLAS (e); and ASAR data (f).

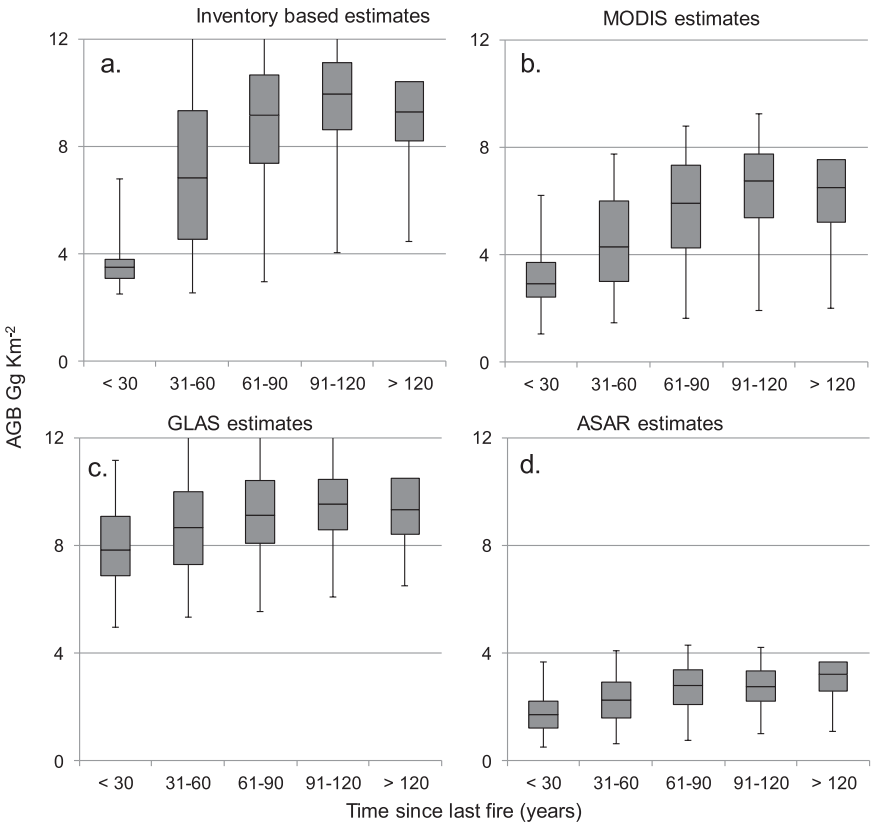

Fig. 10. Box-and-whisker plots of AGB estimates based on inventory data (a), MODIS (b), GLAS (c), and ASAR data (d), as a function of TSLF at the 2-km^2 scale.

canopy structures (Lu et al., 2014) and factors relevant for forest disturbance and recovery patterns (e.g. TSLF, surficial deposits) for AGB estimation.

Acknowledgements

This study was supported by the Fonds Québécois de la Recherche sur la Nature et les Technologies. The Direction des inventaires forestiers, MFFPQ (Ministère de la Forêt, de la Faune et des Parcs du Québec), provided forest inventory plots, forest maps and the SOPFEU fire history map, for which we are grateful. We thank Héloïse Le Goff, Annie-Claude Bélisle and Daniel Lesieur for their fire history maps, and Glenda Russo for helping us to access AGB maps that were based on MODIS data from Canada's National Forest Inventory portal. Martin Thurner graciously provided ASAR biomass estimates. We also thank Marc Simard for freely allowing us to access GLAS canopy height data. Rémi Saint-Amant provided the normal climate database from the NCEP-NCAR Twentieth Century Reanalysis project for the BioSIM simulations. We thank Dr. Mike Wulder (Research Scientist, Pacific Forestry Centre, Natural Resources Canada), Dr. Richard Fournier (Professor, Centre d'Applications et de Recherches en Télédétection, Université de Sherbrooke), Dr. Martin Schlerf (Senior Research Associate in Earth Observation, Luxembourg Institute of Science and Technology) and Dr. Steven Cumming (Professor, Département des sciences du bois et de la forêt, Université Laval) for providing very useful comments on the final version of this manuscript and W.F.J. Parsons (Centre d'Étude de la Forêt) for English editing.

References

Ahmed, O.S., Franklin, S.E., Wulder, M.A., 2014. Interpretation of forest disturbance using a time series of Landsat imagery and canopy structure from airborne lidar. Can. J. Remote Sens. 39 (6), 521–542. http://dx.doi.org/10.5589/m14-004.

Amiro, B.D., Stocks, B.J., Alexander, M.E., Flannigan, M.D., Wotton, B.M., 2001. Fire, climate change, carbon and fuel management in the Canadian boreal forest. Int. J. Wildl. Fire 10 (4), 405–413. http://dx.doi.org/10.1071/WF03066.

Asner, G.P., Clark, J.K., Mascaro, J., Galindo García, G.A., Chadwick, K.D., Navarrete Encinales, D.A., Paez-Acosta, G., Cabrera Montenegro, E., Kennedy-Bowdoin, T., Duque, Á., Balaji, A., von Hildebrand, P., Maatoug, L., Phillips Bernal, J.F., Yepes Quintero, A.P., Knapp, D.E., GarcíaDávila, M.C., Jacobson, J., Ordóñez, M.F., 2012. High-resolution mapping of forest carbon stocks in the Colombian Amazon. Biogeosciences 9 (7), 2683–2696. http://dx.doi.org/10.5194/bg-9-2683-2012.

Asner, G.P., Powell, G.V.N., Mascaro, J., Knapp, D.E., Clark, J.K., Jacobson, J., Kennedy-Bowdoin, T., Balaji, A., Paez-Acosta, G., Victoria, E., Secada, L., Valqui, M., Hughes, R.F., 2010. High-resolution forest carbon stocks and emissions in the Amazon. Proc. Natl. Acad. Sci. 107 (38), 16738–16742. http://dx.doi.org/10.1073/pnas.1004875107.

Avitabile, V., Herold, M., Henry, M., Schmullius, C., 2011. Mapping biomass with remote sensing: a comparison of methods for the case study of Uganda. Carbon Balance Manag. 6 (7), 1–14. http://dx.doi.org/10.1186/1750-0680-6-7.

Baccini, A., Goetz, S.J., Walker, W.S., Laporte, N.T., Sun, M., Sulla-Menashe, D., Hackler, J., Beck, P.S.A., Dubayah, R., Friedl, M.A., Samanta, S., Houghton, R.A., 2012. Estimated carbon dioxide emissions from tropical deforestation improved by carbon-density maps. Nat. Clim. Chang. 2 (3), 182–185. http://dx.doi.org/10.1038/nclimate1354.

Bartels, S.F., Chen, H.Y.H., Wulder, M.A., White, J., 2016. Trends in post-disturbance recovery rates of Canada's forests following wildfire and harvest. For. Ecol. Manag. 361, 194–207. http://dx.doi.org/10.1016/j.foreco.2015.11.015.

Beaudoin, A., Bernier, P.Y., Guindon, L., Villemaire, P., Guo, X.J., Stinson, G., Bergeron, T., Magnussen, S., Hall, R.J., 2014. Mapping attributes of Canada's forests at moderate resolution through *k*NN and MODIS imagery. Can. J. For. Res. 44 (5), 521–532. http://dx.doi.org/10.1139/cjfr-2013-0401.

Bélisle, A.C., Gauthier, S., Cyr, D., Bergeron, Y., Morin, H., 2011. Fire regime and old-growth boreal forests in central Québec, Canada: an ecosystem management perspective. Silva Fenn. 45 (5), 889–908. 〈http://www.silvafennica.fi/pdf/article77.pdf〉.

Bergeron, Y., Gauthier, S., Flannigan, M., Kafka, V., 2004. Fire regimes at the transition between mixedwood and moniferousboreal forest in northwestern Quebec. Ecology 85 (7), 1916–1932. http://dx.doi.org/10.1890/02-0716.

Bergeron, Y., Leduc, A., Harvey, B.D., Gauthier, S., 2002. Natural fire regime: a guide for sustainable management of the Canadian boreal forest. Silva Fenn. 36 (1), 81–95. 〈http://www.metla.eu/silvafennica/full/sf36/sf361081.pdf〉.

Bouchard, M., Pothier, D., Gauthier, S., 2008. Fire return intervals and tree species succession in the North Shore region of eastern Quebec. Can. J. For. Res. 38 (6), 1621–1633. http://dx.doi.org/10.1139/X07-201.

Boudewyn, P., Song, X., Magnussen, S., Gillis, M.D., 2007. Model-based, volume-to-biomass conversion for forested and vegetated land in Canada. Natural Resources Canada Canadian Forest Service, Pacific Forestry Centre, Victoria, BC, Inf. Rep. BC-X-411.

Bradshaw, C.J.A., Warkentin, I.G., 2015. Global estimates of boreal forest carbon stocks and flux. Glob. Planet. Change 128, 24–30. http://dx.doi.org/10.1016/j.gloplacha.

2015.02.004.
Buech, R.R., Rugg, D.J., 1989. Biomass relations of shrub components and their generality. For. Ecol. Manag. 26 (4), 257–264. http://dx.doi.org/10.1016/0378-1127(89)90086-8.
Burkhart, H.E., Tomé, M., 2012. Modeling forest trees and stands. Springer Science & Business Media.
Chaieb, C., Fenton, N.J., Lafleur, B., Bergeron, Y., 2015. Can we use forest inventory mapping as a coarse filter in ecosystem based management in the black spruce boreal forest? Forests 6 (4), 1195–1207. http://dx.doi.org/10.3390/f6041195.
Chave, J., Coomes, D., Jansen, S., Lewis, S.L., Swenson, N.G., Zanne, A.E., 2009. Towards a worldwide wood economics spectrum. Ecol. Lett. 12 (4), 351–366. http://dx.doi.org/10.1016/10.1111/j.1461-0248.2009.01285.x.
Chu, T., Guo, X., 2014. Remote sensing techniques in monitoring post-fire effects and patterns of forest recovery in Boreal forest regions: a review. Remote Sens. 6 (1), 470–520.
Compo, G.P., Whitaker, J.S., Sardeshmukh, P.D., Matsui, N., Allan, R.J., Yin, X., Gleason, B.E., Vose, R.S., Rutledge, G., Bessemoulin, P., Brönnimann, S., Brunet, M., Crouthamel, R.I., Grant, A.N., Groisman, P.Y., Jones, P.D., Kruk, M.C., Kruger, A.C., Marshall, G.J., Maugeri, M., Mok, H.Y., Nordli, Ø., Ross, T.F., Trigo, R.M., Wang, X.L., Woodruff, S.D., Worley, S.J., 2011. The twentieth century reanalysis project. Q. J. Roy. Meteorol. Soc. 137 (654), 1–28. http://dx.doi.org/10.1002/qj.776.
Dormann, F., C, McPherson, M., J, Araújo, B., M, Bivand, R., Bolliger, J., Carl, G., Davies, G., R, Hirzel, A., Jetz, W., Daniel Kissling, W., Kühn, I., Ohlemüller, R., R. Peres-Neto, P., Reineking, B., Schröder, B., M. Schurr, F., Wilson, R., 2007. Methods to account for spatial autocorrelation in the analysis of species distributional data: a review. Ecography 30, 609–628. http://dx.doi.org/10.1111/j.2007.0906-7590.05171.x.
Dormann, C.F., Elith, J., Bacher, S., Buchmann, C., Carl, G., Carré, G., Garcia Marquéz, J.R., Gruber, B., Lafourcade, B., Leitão, P.J., Münkemüller, T., McClean, C., Osborne, P.E., Reineking, B., Schröder, B., Skidmore, A.K., Zurell, D., Lautenbach, S., 2013. Collinearity: a review of methods to deal with it and a simulation study evaluating their performance. Ecography 36 (1), 27–46. http://dx.doi.org/10.1111/j.1600-0587.2012.07348.x.
Drake, J.B., Knox, R.G., Dubayah, R.O., Clark, D.B., Condit, R., Blair, J.B., Hofton, M., 2003. Above-ground biomass estimation in closed canopy Neotropical forests using lidar remote sensing: factors affecting the generality of relationships. Glob. Ecol. Biogeogr. 12 (2), 147–159. http://dx.doi.org/10.1046/j.1466-822X.2003.00010.x.
Dunne, T., Leopold, L.B., 1978. Water in Environmental Planning, 1st ed. W.H. Freeman & Company, San Francisco, pp. 566–580.
FAO, 2015. Global Forest Resources Assessment 2015. How are the world's forests changing?. ⟨http://www.fao.org/3/a-i4793e.pdf⟩. (accessed 29 October 2015).
Frelich, L.E., Reich, P.B., 1999. Neighborhood effects, disturbance severity, and community stability in forests. Ecosystems 2 (2), 151–166. http://dx.doi.org/10.1007/s100219900066.
Frolking, S., Palace, M.W., Clark, D.B., Chambers, J.Q., Shugart, H.H., Hurtt, G.C., 2009. Forest disturbance and recovery: a general review in the context of spaceborne remote sensing of impacts on aboveground biomass and canopy structure. J. Geophys. Res. -Biogeo. 114, G2. http://dx.doi.org/10.1029/2008JG000911.
Gauthier, S., Boucher, D., Morissette, J., De Grandpré, L., 2010. Fifty-seven years of composition change in the eastern boreal forest of Canada. J. Veg. Sci. 21, 772–785. http://dx.doi.org/10.1111/j.1654-1103.2010.01186.x.
Gillis, M.D., Omule, A.Y., Brierley, T., 2005. Monitoring Canada's forests: the National Forest Inventory. For. Chron. 81 (2), 214–221. http://dx.doi.org/10.5558/tfc81214-2.
Girardin, M.P., Ali, A.A., Carcaillet, C., Gauthier, S., Hely, C., Le Goff, H., Terrier, A., Bergeron, Y., 2013. Fire in managed forests of eastern Canada: risks and options. For. Ecol. Manag. 294, 238–249. http://dx.doi.org/10.1016/j.foreco.2012.07.005.
Gower, S.T., Vogel, J.G., Norman, J.M., Kucharik, C.J., Steele, S.J., Stow, T.K., 1997. Carbon distribution and aboveground net primary production in aspen, jack pine, and black spruce stands in Saskatchewan and Manitoba, Canada. J. Geophys. Res. Atmos. 102 (D24), 29029–29041. http://dx.doi.org/10.1029/97JD02317.
Harden, J.W., Trumbore, S.E., Stocks, B.J., Hirsch, A., Gower, S.T., O'neill, K.P., Kasischke, E.S., 2000. The role of fire in the boreal carbon budget. Glob. Chang. Biol. 6 (S1), 174–184. http://dx.doi.org/10.1046/j.1365-2486.2000.06019.x.
Hill, T.C., Williams, M., Bloom, A.A., Mitchard, E.T., Ryan, C.M., 2013. Are inventory based and remotely sensed above-ground biomass estimates consistent? PLoSONE 8 (9), e74170. http://dx.doi.org/10.1371/journal.pone.0074170.
Houghton, R.A., 2005. Aboveground forest biomass and the global carbon balance. Glob. Chang. Biol. 11 (6), 945–958. http://dx.doi.org/10.1111/j.1365-2486.2005.00955.x.
Irulappa Pillai Vijayakumar, Raulier, D.B., Bernier, F., Gauthier, P.Y., Bergeron, S., Y., Pothier, D., 2015. Lengthening the historical records of fire history over large areas of boreal forest in eastern Canada using empirical relationships.For. Ecol. Manag. 347, 30–39. http://dx.doi.org/10.1016/j.foreco.2015.03.011.
Irulappa Pillai Vijayakumar, Raulier, D.B., Bernier, F., Paré, P.Y., Gauthier, D., Bergeron, S., Y., Pothier, D., 2016. Cover density recovery after fire disturbance controls landscape aboveground carbon biomass in the boreal forest of eastern Canada. For. Ecol. Manag. 360, 170–180. http://dx.doi.org/10.1016/j.foreco.2015.10.035.
Jin, Y., Randerson, J.T., Goetz, S.J., Beck, P.S., Loranty, M.M., Goulden, M.L., 2012. The influence of burn severity on postfire vegetation recovery and albedo change during early succession in North American boreal forests. J. Geophys. Res. -Biogeo. 117 (G1), G01036. http://dx.doi.org/10.1029/2011JG001886.
Jones, M.O., Kimball, J.S., Jones, L.A., 2013. Satellite microwave detection of boreal forest recovery from the extreme 2004 wildfires in Alaska and Canada. Glob. Change Biol. 19 (10), 3111–3122. http://dx.doi.org/10.1111/gcb.12288.
Johnson, E.A., Gutsell, S.L., 1994. Fire frequency models, methods and interpretations. Adv. Ecol. Res. 25, 239–287.
Johnson, E.A., Miyanishi, K., Weir, J.M.H., 1998. Wildfires in the Western Canadian Boreal Forest: landscape patterns and ecosystem management. J. Veg. Sci. 9, 603–610. ⟨http://www.jstor.org/stable/3237276⟩.
Johnstone, J.F., Hollingsworth, T.N., Chapin III, F.S., Mack, M.C., 2010. Changes in fire regime break the legacy lock on successional trajectories in Alaskan boreal forest. Glob. Change Biol. 16 (4), 1281–1295. http://dx.doi.org/10.1111/j.1365-2486.2009.02051.x.
Kursa, M.B., Rudnicki, W.R., 2010. Feature selection with the Boruta package. J. Stat. Softw. 36, 1–13. ⟨http://www.jstatsoft.org/v36/i11⟩.
Lambert, M.C., Ung, C.-H., Raulier, F., 2005. Canadian national tree above ground biomass equations. Can. J. For. Res. 35 (8), 1996–2018. http://dx.doi.org/10.1139/x05-112.
Lecomte, N., Simard, M., Fenton, N., Bergeron, Y., 2006. Fire severity and long-term ecosystem biomass dynamics in coniferous boreal forests of eastern Canada. Ecosystems 9 (8), 1215–1230. http://dx.doi.org/10.1007/s10021-004-0168-x.
Le Goff, H., Flannigan, M.D., Bergeron, Y., Girardin, M.P., 2007. Historical fire regime shifts related to climate teleconnections in the Waswanipi area, central Quebec, Canada. Int. J. Wildland Fire 16 (5), 607–618. http://dx.doi.org/10.1071/WF06151.
Lesieur, D., Gauthier, S., Bergeron, Y., 2002. Fire frequency and vegetation dynamics for the south-central boreal forest of Quebec, Canada. Can. J. For. Res. 32 (11), 1996–2009. http://dx.doi.org/10.1139/x02-113.
Liaw, A., Wiener, M., 2002. Classification and regression by random. Forest R news 2 (3), 18–22.
Lu, D., Chen, Q., Wang, G., Liu, L., Li, G., Moran, E., 2014. A survey of remote sensing-based aboveground biomass estimation methods in forest ecosystems. Int. J. Digit. Earth 1–43. http://dx.doi.org/10.1080/17538947.2014.990526.
McGuire, A.D., 2002. Ecosystem element cycling. In: El-shaarawi, A.H., Piegorsch, W.W. (Eds.), Encyclopedia of Environmetrics. John Wiley and Sons Ltd., Chichester, UK, pp. 614–618.
Madoui, A., Gauthier, S., Leduc, A., Bergeron, Y., Valeria, O., 2015. Monitoring forest recovery following wildfire and harvest in boreal forests using satellite imagery. Forests 6 (11), 4105–4134. http://dx.doi.org/10.3390/f6114105.
Magnussen, S., Tomppo, E., McRoberts, R.E., 2010. A model-assisted k-nearest neighbour approach to remove extrapolation bias. Scand. J. For. Res. 25 (2), 174–184. http://dx.doi.org/10.1080/02827581003667348.
Main-Knorn, M., Moisen, G.G., Healey, S.P., Keeton, W.S., Freeman, E.A., Hostert, P., 2011. Evaluating the remote sensing and inventory-based estimation of biomass in the Western Carpathians. Remote Sens. 3 (7), 1427–1446. http://dx.doi.org/10.3390/rs3071427.
Main-Knorn, M., Cohen, W.B., Kennedy, R.E., Grodzki, W., Pflugmacher, D., Griffiths, P., Hostert, P., 2013. Monitoring coniferous forest biomass change using a Landsat trajectory-based approach. Remote Sens. Environ. 139, 277–290. http://dx.doi.org/10.1016/j.rse.2013.08.010.
Malhi, Y., 2012. The productivity, metabolism and carbon cycle of tropical forest vegetation. J. Ecol. 100 (1), 65–75. http://dx.doi.org/10.1111/j.1365-2745.2011.01916.x.
Malhi, Y., Phillips, O.L., Lloyd, J., Baker, T., Wright, J., Almeida, S., et al., 2002. An international network to monitor the structure, composition and dynamics of Amazonian forests (RAINFOR). J. Veg. Sci. 13 (3), 439–450. http://dx.doi.org/10.1658/1100-9233(2002)013[0439:AINTMT]2.0.CO;2.
Mansuy, N., Gauthier, S., Robitaille, A., Bergeron, Y., 2010. The effects of surficial deposit–drainage combinations on spatial variations of fire cycles in the boreal forest of eastern Canada. Int. J. Wildland Fire 19 (8), 1083–1098. http://dx.doi.org/10.1071/WF09144.
Mansuy, N., Gauthier, S., Robitaille, A., Bergeron, Y., 2012. Regional patterns of postfire canopy recovery in the northern boreal forest of Quebec: interactions between surficial deposit, climate, and fire cycle. Can. J. For. Res. 42 (7), 1328–1343. http://dx.doi.org/10.1139/x2012-101.
Mansuy, N., Thiffault, E., Lemieux, S., Manka, F., Paré, D., Lebel, L., 2015. Sustainable biomass supply chains from salvage logging of fire-killed stands: a case study for wood pellet production in eastern Canada. Appl. Energy 154, 62–73. http://dx.doi.org/10.1016/j.apenergy.2015.04.048.
Margolis, H.A., Nelson, R.F., Montesano, P.M., Beaudoin, A., Sun, G., Andersen, H.-E., Wulder, M.A., 2015. Combining satellite lidar, airborne lidar, and ground plots to estimate the amount and distribution of aboveground biomass in the boreal forest of North America. Can. J. For. Res. 45, 838–855. http://dx.doi.org/10.1139/cjfr-2015-0006.
Mitchard, E.T., Feldpausch, T.R., Brienen, R.J., Lopez-Gonzalez, G., Monteagudo, A., Baker, T.R., et al., 2014. Markedly divergent estimates of Amazon forest carbon density from ground plots and satellites. Glob. Ecol. Biogeogr. 23, 935–946. http://dx.doi.org/10.1016/10.1111/geb.12168.
Mitchard, E.T., Saatchi, S.S., Baccini, A., Asner, G.P., Goetz, S.J., Harris, N.L., Brown, S., 2013. Uncertainty in the spatial distribution of tropical forest biomass: a comparison of pan-tropical maps. Carbon Balance Manag. 8, 1–13. http://dx.doi.org/10.1186/1750-0680-8-10.
Neigh, C.S., Nelson, R.F., Ranson, K.J., Margolis, H.A., Montesano, P.M., Sun, G., et al., 2013. Taking stock of circumboreal forest carbon with ground measurements, airborne and spaceborne LiDAR. Remote Sens. Environ. 137, 274–287. http://dx.doi.org/10.1016/j.rse.2013.06.019.
Pan, Y., Birdsey, R.A., Fang, J., Houghton, R., Kauppi, P.E., Kurz, W.A., Phillips, O.L., Shvidenko, A., Lewis, S.L., Canadell, J.G., Ciais, P., Jackson, R.B., Pacala, S.W., McGuire, A.D., Piao, S., Rautiainen, A., Sitch, S., Hayes, D., 2011. A large and persistent carbon sink in the World's forests. Science 333 (6045), 988–993. http://dx.doi.org/10.1126/science.1201609.
Pelletier, G., Dumont, Y., Bédard, M., 2007. SIFORT: Système d'Information FORestière par Tesselle, Manuel de l'usager. Ministère des Ressources naturelles etde la Faune du Québec, Québec, QC, Canada. ⟨https://www.mffp.gouv.qc.ca/publications/forets/

fimaq/usager.pdf〉 (accessed 2.10. 2014).
Pflugmacher, D., Cohen, W., Kennedy, R., Lefsky, M., 2008. Regional applicability of forest height and aboveground biomass models for the geoscience laser Altimeter system. For. Sci. 54 (6), 647–657.
Pflugmacher, D., Cohen, W.B., Kennedy, R.E., 2012. Using Landsat-derived disturbance history (1972–2010) to predict current forest structure. Remote Sens. Environ. 122, 146–165. http://dx.doi.org/10.1016/j.rse.2011.09.025.
Pflugmacher, D., Cohen, W.B., Kennedy, R.E., Yang, Z., 2014. Using Landsat-derived disturbance and recovery history and lidar to map forest biomass dynamics. Remote Sens. Environ. 151, 124–137. http://dx.doi.org/10.1016/j.rse.2013.05.033.
Régnière, J., St-Amant, R., 2008. BioSIM 9 user's manual. Natural Resources Canada, Canadian Forest Service, Laurentian Forestry Centre, Quebec, QC, Canada (Information Report LAU-X-134E). 〈https://cfs.nrcan.gc.ca/publications?id=28768〉 (accessed 7.10. 2014).
Robitaille, A., Saucier, J.-P., 1998. Paysages régionaux du Québec méridional. Direction de la gestion des stocks forestiers et Direction des relations publiques, ministère des Ressources naturelles du Québec. Les publications du Québec, Québec.
Saucier, J.-.P., Grondin, P., Robitaille, A., Gosselin, J., Morneau, C., Richard, P.J.H., Brisson, J., Sirois, L., Leduc, A., Morin, H., Thiffault, E., Gauthier, S., Lavoie, C., Payette, S., 2009. Écologie forestière - Chapitre 4. pp. 167–315 Manuel de Foresterie (2ème édition). Éditions M. Québec.
Santoro, M., Beer, C., Cartus, O., Schmullius, C., Shvidenko, A., McCallum, I., Wegmüller, U., Wiesmann, A., 2011. Retrieval of growing stock volume in boreal forest using hyper-temporal series of Envisat ASAR ScanSAR backscatter measurements. Remote Sens. Environ. 115 (2), 490–507. http://dx.doi.org/10.1016/j.rse.2010.09.018.
Saatchi, S.S., Harris, N.L., Brown, S., Lefsky, M., Mitchard, E.T., Salas, W., et al., 2011. Benchmark map of forest carbon stocks in tropical regions across three continents. Proc. Natl. Acad. Sci. 108 (24), 9899–9904. http://dx.doi.org/10.1073/pnas.1019576108.
Simard, M., Pinto, N., Fisher, J.B., Baccini, A., 2011. Mapping forest canopy height globally with spaceborne lidar. J. Geophys. Res. Biogeosci. 116 (G4), G04021. http://dx.doi.org/10.1029/2011JG001708.
Ter-Mikaelian, M.T., Korzukhin, M.D., 1997. Biomass equations for sixty-five North American tree species. For. Ecol. Manag. 97 (1), 1–24. http://dx.doi.org/10.1016/S0378-1127(97)00019-4.
Thompson, J.R., Spies, T.A., 2009. Vegetation and weather explain variation in crown damage within a large mixed-severity wildfire. For. Ecol. Manag. 258 (7), 1684–1694. http://dx.doi.org/10.1016/j.foreco.2009.07.031.
Thurner, M., Beer, C., Santoro, M., Carvalhais, N., Wutzler, T., Schepaschenko, D., Shvidenko, A., Kompter, E., Ahrens, B., Levick, S.R., Schmullius, C., 2014. Carbon stock and density of northern boreal and temperate forests. Glob. Ecol. Biogeogr. 23 (3), 297–310. http://dx.doi.org/10.1016/10.1111/geb.12125.
Ung, C.H., Bernier, P., Guo, X.-J., 2008. Canadian national biomass equations: new parameter estimates that include British Columbia data. Can. J. For. Res. 38 (5), 1123–1132. http://dx.doi.org/10.1139/X07-224.
Van Zyl, J.J., 2001. The Shuttle Radar Topography Mission (SRTM): a breakthrough in remote sensing of topography. Acta Astronautica 48 (5), 559–565. http://dx.doi.org/10.1016/S0094-5765(01)00020-0.
Zhang, G., Ganguly, S., Nemani, R.R., White, M.A., Milesi, C., Hashimoto, H., Wang, W., Saatchi, S., Yu, Y., Myneni, R.B., 2014a. Estimation of forest aboveground biomass in California using canopy height and leaf area index estimated from satellite data. Remote Sens. Environ. 151, 44–56. http://dx.doi.org/10.1016/j.rse.2014.01.025.
Zhang, J., Huang, S., Hogg, E.H., Lieffers, V.J., Qin, Y., He, F., 2014b. Estimating spatial variation in Alberta forest biomass from a combination of forest inventory and remote sensing data. Biogeosciences 11 (10), 2793–2808. http://dx.doi.org/10.5194/bg-11-2793-2014.
Zhao, K., Popescu, S., Nelson, R., 2009. Lidar remote sensing of forest biomass: a scale-invariant estimation approach using airborne lasers. Remote Sens. Environ. 113 (1), 182–196. http://dx.doi.org/10.1016/j.rse.2008.09.009.
Zolkos, S.G., Goetz, S.J., Dubayah, R., 2013. A meta-analysis of terrestrial aboveground biomass estimation using lidar remote sensing. Remote Sens. Environ. 128, 289–298. http://dx.doi.org/10.1016/j.rse.2012.10.017.